Vietnam Journal of Science and Technology ***62*** *(3) (2024) 486-495*

doi:10.15625/2525-2518/17553

Curing process, mechanical property and thermal stability of acrylic polyurethane/Fe_2O_3 nanocomposite coatings

Do Truc Vy[1, 2], Dao Phi Hung[1, 2], Nguyen Tuan Anh[1], Tran Dai Lam[1, 2], Nguyen Thien Vuong[1, 2, *]

[1]*Institute for Tropical Technology, Vietnam Academy of Science and Technology, 18 Hoang Quoc Viet, Cau Giay, Ha Noi, Viet Nam*

[2]*Graduate University of Science and Technology, Vietnam Academy of Science and Technology, 18 Hoang Quoc Viet, Cau Giay, Ha Noi, Viet Nam*

[*]Emails: *vuongvast@gmail.com*

Received: 4 October 2022; Accepted for publication: 5 December 2022

Abstract. The effects of Fe_2O_3 nanoparticles (NPs) on the curing and properties of acrylic polyol HSU 1168-based coatings were investigated. SEM images showed that Fe_2O_3 NPs with a content of ≤ 2 wt.% were regularly dispersed in the polymer matrix. The results indicated that Fe_2O_3 NPs slowed the curing process of the acrylic polyol coating. Without NPs, the neat HSU 1168-based coating cured completely after 96 hours, whereas with 2 wt.% Fe_2O_3 NPs, 120 hours were required. Additionally, Fe_2O_3 NPs had a negligible effect on the relative hardness at low contents. However, at higher contents (> 2 wt.%), the relative hardness decreased as the Fe_2O_3 NP content increased from 2 to 4 wt.%. Without nanoparticles, the relative hardness of the neat acrylic polyol coating was 0.88, compared to 0.75 with 4 wt.% Fe_2O_3 NPs. Furthermore, 2 wt.% Fe_2O_3 NPs enhanced abrasion resistance (180.5 L/mil) and impact resistance (200 kg.cm). Incorporating Fe_2O_3 NPs also improved thermal stability, with degradation starting 15 °C higher than in the neat coating.

Keyword: acrylic polyol coating, nanocomposite coating, Fe_2O_3 nanoparticles, thermal stability, mechanical properties.

Classification number: 2.5.3

1. INTRODUCTION

Polymer composite coatings are used as protective and decorative materials for various substrates and must meet strict standards. They require good weather durability, high mechanical properties, and special functionalities such as anticorrosion protection and antimicrobial performance. Nanotechnology appears promising in addressing these challenges. Compared to microparticles in pigments, NPs exhibit superior performance even at small concentrations (e.g., 1 - 5 wt.%) [1]. NPs have been incorporated into organic coatings to enhance various properties including weather durability [2-4], chemical resistance [5, 6], mechanical strength [7, 8], antimicrobial activity [8, 9], anti-corrosion protection [10], and self-cleaning capabilities [11, 12].

Among inorganic NPs, ferric oxide NPs could enhance mechanical properties, UV durability, chemical resistance, etc. of organic coatings. Jin and his co-workers investigated the effect of Fe_2O_3 NPs content, i.e. 2.5 wt.%, 5 wt.% and 7.5 wt.%, on the anti-corrosion protection of epoxy coatings on magnesium alloys [13]. The epoxy coating filled with 5 wt.% Fe_2O_3 NPs had the highest adhesion strength value. Tafel tests indicated more positive corrosion potential and lower corrosion current density with increasing Fe_2O_3 content. However, at Fe_2O_3 NPs content higher than 5.0 wt.%, the anti-corrosion activity decreased [13]. In order to enhance the anti-corrosion protection of the epoxy coating, Chen and his colleagues used tannic acid and graphene oxide-modified Fe_2O_3 NPs [14]. Their findings showed that the maximum corrosion resistance of the composite coating was achieved when 5 wt.% modified Fe_2O_3 was added. The epoxy coating filled with 5 wt.% modified Fe_2O_3 had a charge transfer resistance of 14350 $\Omega.cm^2$ and a corrosion current density of 1.459 $\mu A/cm^2$ [14]. Liu *et al.* reported the results of preparing a self-healing epoxy coating filled with tetraaniline-modified α-Fe_2O_3 NPs [15]. The epoxy coating containing 0.7 wt.% modified α-Fe_2O_3 NPs had superior corrosion resistant property, strong adhesion force, low water absorption, low O_2 permeability and good salt spray resistance. Graphene oxide-modified Fe_2O_3 was also confirmed to enhance the anticorrosion performance of epoxy coatings [16]. Besides, the incorporation of nano Fe_2O_3 into the coating matrix enhanced its UV resistance, acid/alkali resistance, and color stability [17].

Acrylic polyol resin has been widely used as a binder for organic coatings thanks to its good properties such as high weather durability [18] and good mechanical properties [19] (good adhesion, high impact resistance, etc.). It was reported that the properties of acrylic polyol-based coatings could be enhanced by the addition of UV absorbance agents or TiO_2 NPs. However, in order to diverse the application of acrylic polyol-based composite coatings, this work aims to reveal the effect of Fe_2O_3 NPs on curing process, mechanical properties and thermal stability of acrylic polyol-based coatings.

2. EXPERIMENTAL

2.1. Materials

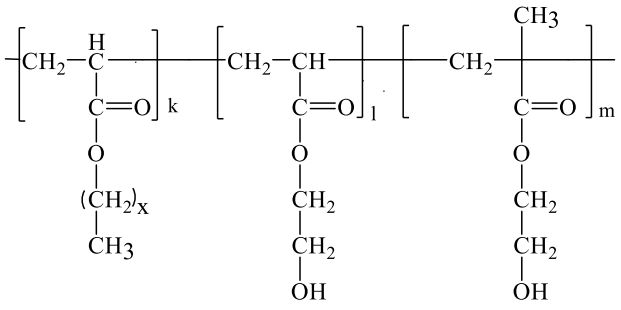

where, k, l, m: 0, 1, 2, 3, …; x: 0, 1, 2 ,3.

Diagram 1. Formula of HSU 1168 resin.

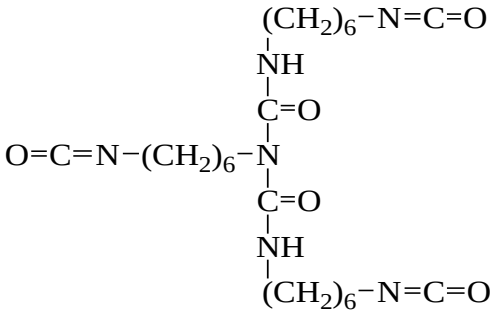

Diagram 2. Formula of Desmodur N.75.

Acrylic polyol resin HSU 1168 solution (solid content of 65 wt.%) with a hydroxyl content of 4.3 wt.% (based on solid part) was obtained from Add and Poly Resin Industrial Co., Ltd. (Taiwan). The formula of HSU 1168 is presented in Diagram 1. Polyisocyanate (tradename is

Desmodur N.75) (PI) with an isocyanate content of 17 wt.% was purchased from Bayer (Germany). PI solution had 75 wt.% solid fraction. Desmodur N.75's formula is illustrated in Diagram 2. Other chemicals such as P grade toluene and xylene were purchased from Xilong Chemical Co., Ltd. (China).

Fe_2O_3 NPs were supplied by Sigma-Aldrich with an average size of 5 - 25 nm and a specific surface area of 30 m^2/g. Due to their low specific surface area, SEM and TEM images of these Fe_2O_3 NPs (Figure 1) showed that a part of them linked together to form agglomerates with a larger average size (100 nm).

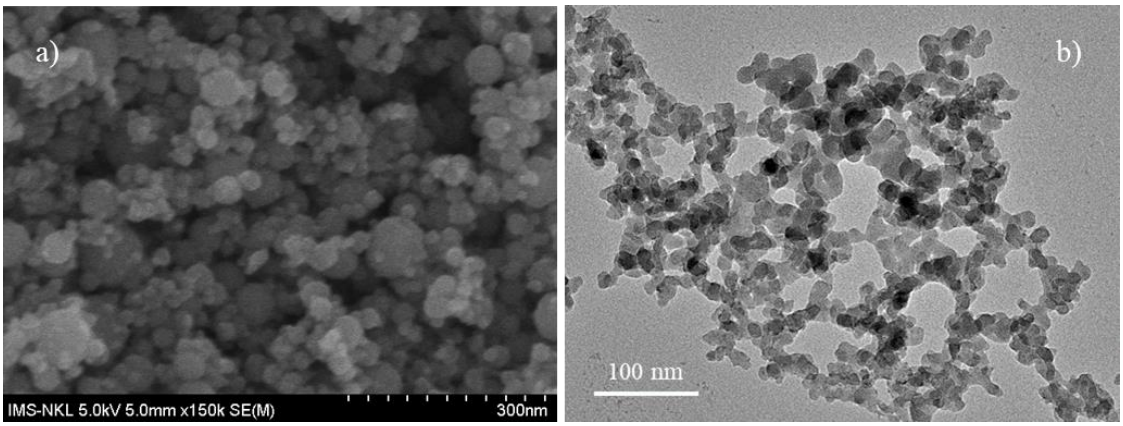

Figure 1. SEM image (a) and TEM image (b) of Fe_2O_3 NPs.

2.2. Sample preparation

The Fe_2O_3 NPs were dispersed in toluene and xylene solution (weight ratio of toluene/xylene = 1/1) by ultrasonication (model TPC-15H, 35 kHz, Telsonic AG, Switzerland) for 2 hours with a weight ratio of Fe_2O_3NPs/solvent = 1/10. Then, the HSU was added to the suspension. The mixture was vibrated by ultrasonication for 1 hour, which was followed by introducing N75 into the mixture. Toluene and xylene solvents with a weight ratio of 1/1 were then introduced to obtain a solid sample at 50 wt.%. The samples were stirred at 300 rpm for 10 minutes. The samples' composition is illustrated in Table 1.

Table 1. Sample composition by weight ratio.

No	Sample	HSU 1168	N.75	Fe_2O_3 NPs	Toluene	Xylene
1	ACPU	30	17.9	0	9.0	9.0
2	ACPU-0.5 % Fe_2O_3	30	17.9	0.17	9.1	9.1
3	ACPU-1 % Fe_2O_3	30	17.9	0.33	9.15	9.15
4	ACPU-2 % Fe_2O_3	30	17.9	0.66	9.3	9.3
5	ACPU-4 % Fe_2O_3	30	17.9	1.32	9.6	9.6

Samples for IR analysis were prepared on KBr pellets with a wet thickness of 20 µm using a spiral film applicator (Erichsen model 358). Samples for hardness measurement and abrasion

resistance determination were prepared on glass substrates with a wet thickness of 120 µm using a film applicator (model 306). Samples for impact resistance and adhesion measurement were fabricated on steel substrates (C45) with a wet thickness of 120 µm. The coatings were hardened for 7 days under natural conditions and then were conditioned for at least 2 days at 25 ^{o}C and 50 % relative humidity before each test. All measurements were conducted three times to obtain the average value.

2.3. Characterization

2.3.1. Infrared spectroscopy analysis

The functional chemical changes of the coating upon curing process were analyzed by Fourier transform infrared (FTIR) spectroscopy (Nicolet NEXUS 670) with a DTGS-KBr detector, resolution of 4 cm^{-1} and 16 scans. The variation bands at 2273 cm^{-1} corresponding to the isocyanate group were quantitatively monitored through discrete measurements performed on exactly the same spot of each sample, after various times. Based on the decrease in absorption intensity, the relative amount of remaining functional groups was determined by the ratio of the IR absorbance after a certain time (D_t) to the absorbance of the initial sample (D_0): remaining group (%) = $(D_t*100)/D_0$.

2.3.2. Mechanical properties

Mechanical properties, i.e. relative hardness, impact resistance, adhesion and abrasion resistance of the samples were measured according to compatible standards, namely ISO 1522, ISO 6272-1, ISO 2409 and ASTM D968, respectively.

2.3.3. Thermal stability

Thermal stability of the samples was determined by thermogravimetric analysis (TGA) using TG209F1 (NETZSCH, Germany) with a heating rate of 10 ^{o}C in air atmosphere.

2.3.4. Morphological study

Morphology of the samples was determined by SEM images of the sample cross-section using FE-SEM S4800 (Hitachi, Japan). To enhance the electro-conductivity of the samples, the sample surface was coated with a very thin layer of Pt.

3. RESULTS AND DISCUSSION

3.1. Effect of Fe_2O_3 NPs on mechanical property of acrylic polyol coating

The effect of Fe_2O_3 NPs content on mechanical properties, i.e. relative hardness, adhesion, abrasion resistance and impact resistance of acrylic polyol coatings was investigated. Coatings with varying Fe_2O_3 NPs contents (0, 0.5, 1, 2, and 4 wt.%) were fully cured after 7 days and conditioned for at least 2 days at 25°C and 50 % relative humidity before testing, as per our previous study [18]. Table 2 summarizes the mechanical properties of these coatings.

Fe_2O_3 NPs had minimal impact on the relative hardness and adhesion of acrylic polyol coatings at low concentrations (≤ 2 wt.%). However, at higher Fe_2O_3 NPs content (4 wt.%), both

relative hardness and adhesion slightly decreased. Conversely, abrasion resistance and impact resistance increased as Fe_2O_3 NPs content rose from 0.5 to 2 wt.%, but declined when the content increased from 2 wt.% to 4 wt.%. This trend aligns with findings from our prior research on rutile TiO_2 NPs. At lower concentrations, NPs dispersed effectively within the polymer matrix, but higher concentrations led to increased NPs density and agglomeration, reducing interphase interaction and subsequently, mechanical properties. ACPU-2 % Fe_2O_3 exhibited the most favorable mechanical properties and was selected for further investigation [19].

Table 2. Mechanical properties of acrylic polyol-based coatings loaded with different Fe_2O_3 NPs contents.

No	Sample	Relative hardness	Adhesion (point)	Abrasion resistance (L/mil)	Impact resistance (kG.cm)
1	ACPU	0.88 ± 0.04	0	132 ± 5	180 ± 5
2	ACPU-0.5 % Fe_2O_3	0.87 ± 0.04	0	159.2 ± 5	185 ± 5
3	ACPU-1 % Fe_2O_3	0.86 ± 0.04	0	166.5 ± 5	190 ± 5
4	ACPU-2 % Fe_2O_3	0.85 ± 0.04	0	180.5 ± 5	≥ 200
5	ACPU-4 % Fe_2O_3	0.75 ± 0.04	1	157.9 ± 5	185 ± 5

3.2. Morphological study

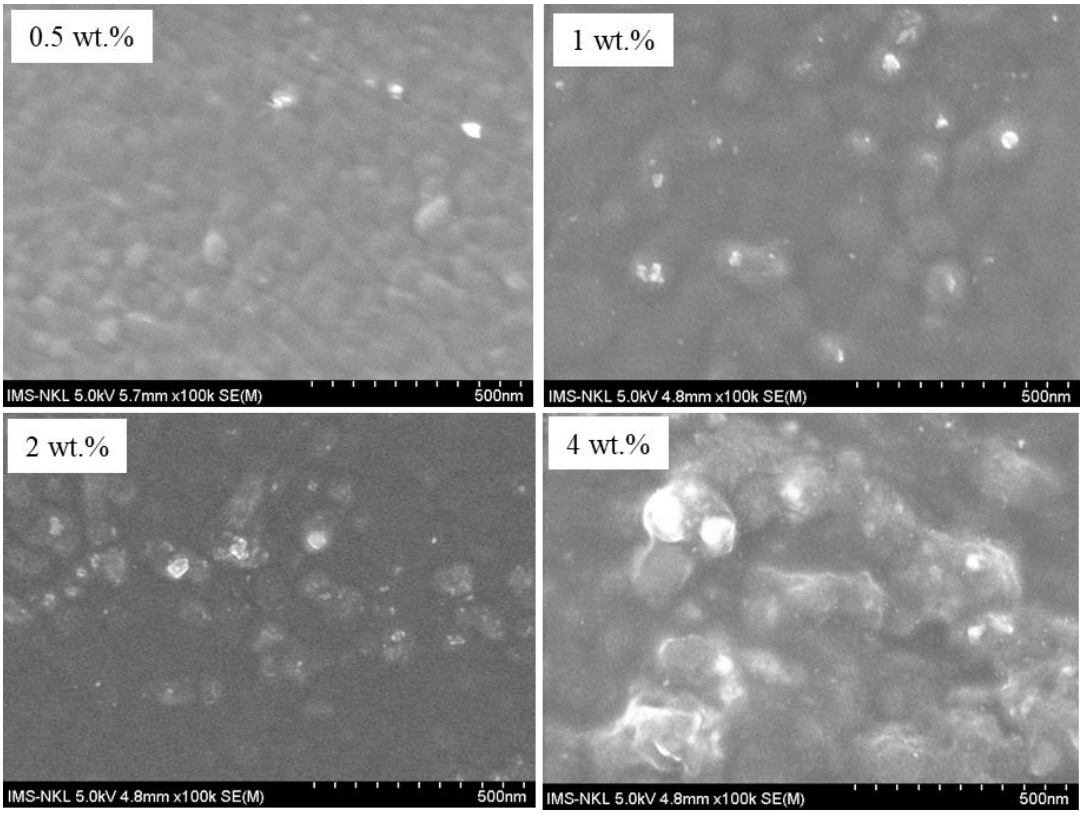

Figure 2. FE-SEM images of ACPU coating filled with 0.5, 1, 2 and 4 wt.% Fe_2O_3 NPs.

Figure 2 displays FE-SEM images of ACPU coatings incorporating 0.5, 1, 2, and 4 wt.% Fe_2O_3 NPs. At Fe_2O_3 NPs concentrations ≤ 2 wt.%, homogeneous dispersion within the ACPU coating matrix is observed, with average agglomerate size around 100 nm. However, at higher Fe_2O_3 NPs concentration (4 wt.%), agglomeration is more pronounced, resulting in larger agglomerate size within the ACPU coating matrix. Consequently, the mechanical properties of the ACPU-4 % Fe_2O_3 coating are inferior to those of other nanocomposite coatings with lower Fe_2O_3 NPs concentrations (see Table 2)

3.3. Effect of Fe_2O_3 NPs on the curing process of ACPU coating

Infrared (IR) spectroscopy is a sensitive physicochemical analysis method commonly employed to track changes in functional groups within materials during chemical processes. In this study, IR analysis was utilized to monitor chemical changes in acrylic polyol-based coatings throughout the curing process. The IR spectra of the acrylic polyol-based coatings at the beginning and after 144 hours are presented in Figure 3.

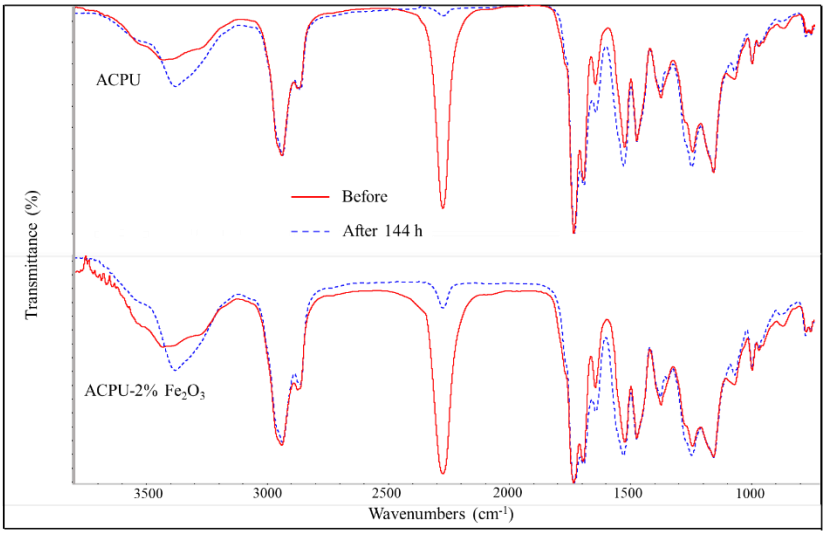

Figure 3. IR spectra of acrylic polyol-based coatings, before and after (144 hours) curing, with or without 2 wt.% Fe_2O_3 NPs.

As can be seen in Figure 3, there are no difference in IR spectra between ACPU-2 % Fe_2O_3 and ACPU. The IR spectra of ACPU-2 % Fe_2O_3 and ACPU had the same absorbance bands. For example, the absorptions located at 3440, 2850, 2273 and 1640 cm^{-1} corresponding to –O-H linkages, C-H linkages (alkane), -N=C=O linkages and C=C linkages, respectively. It can be said that the addition of Fe_2O_3 NPs did not affect the IR spectra of the acrylic polyol coatings. However, in comparison with the IR spectra of the initial coating, the intensity of some peaks of the cured coating changed. The absorption intensity at around 3440 cm^{-1} was increased and the peak absorbance moved to lower wavenumbers, while the vibration intensity of the bands located at 2273 cm^{-1} was decreased. It was explained by the reaction of isocyanate and hydroxyl groups:

Therefore, the absorbance of the OH linkages and isocyanate decreased while the vibration of the N-H linkages increased. It was difficult to distinguish between OH linkage absorbance and N-H linkage absorbance, so the vibration of the NCO linkage located at 2273 cm^{-1} was chosen for quantitative analysis. The change of the isocyanate group is displayed in Figure 4.

It can be seen from Figure 4 that the isocyanate content decreased sharply during the first 72 hours of the curing process. Then, the isocyanate content decreased slowly and remained unchanged after 120 hours. In comparison with the ACPU coating, the ACPU-2 % Fe_2O_3 had a lower speed of curing. This result agreed with the ACPU coating in the presence of a photostabilizer [18]. The presence of strange agents such as NPs and photostabilizers may reduce intergroup interactions and system mobility. Thus, the chemical conversion of the coating decreased. It can be said that the chemical conversion of the acrylic polyol-based coatings was completed after 120 hours. However, the completion of the chemical conversion did not mean that the hardening process was complete. Therefore, changes in the relative hardness of the coatings over time were investigated and the results obtained are illustrated in Figure 4.

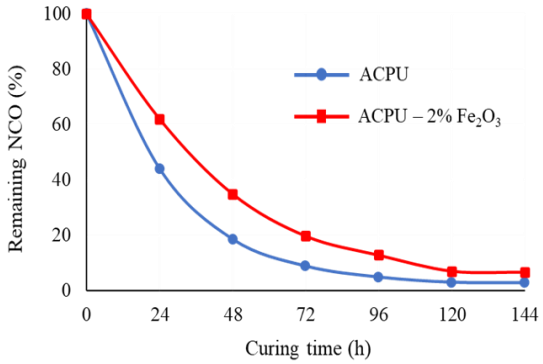

Figure 4. Changes in isocyanate content during curing process.

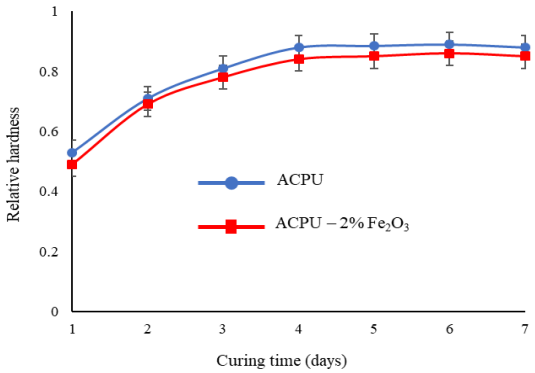

Figure 5. Changes in relative hardness of ACPU and ACPU-2 % Fe_2O_3.

As can be seen from Figure 5, the relative hardness of the coatings increased rapidly during the first 4 days, and then increased slowly and remained stable after 5 days. After 7 days, the relative hardness of ACPU and ACPU-2 % Fe_2O_3 reached 0.88 and 0.85, respectively. It can be said that the acrylic polyol-based nanocomposite coatings hardened completely after 5 days.

3.5. Thermal stability

TGA curves of ACPU and ACPU-2 % Fe_2O_3 coatings are presented in Figure 6. TGA parameters such as T_5, T_{50} and T_{75} (corresponding to the temperature at which the coating lost 5 wt.%, 50 wt.% and 75 wt.%, respectively) are illustrated in Table 3.

As can be seen from Figure 6, the ACPU and ACPU-2 % Fe_2O_3 coatings had similar TGA curves. The weight of the coating was stable during the first period of heating, then the weight of the coating started losing from over 200 ^oC. In the literature, the temperature at which the weight of a material loses 5 wt.% is usually considered the onset temperature of degradation. The weight of the coating lost sharply with continuous increase of temperature. Finally, the weight of the coating did not change at temperatures over 600 ^oC. The residual weight of ACPU-2 % Fe_2O_3 was higher than that of ACPU, possibly due to the addition of Fe_2O_3 NPs.

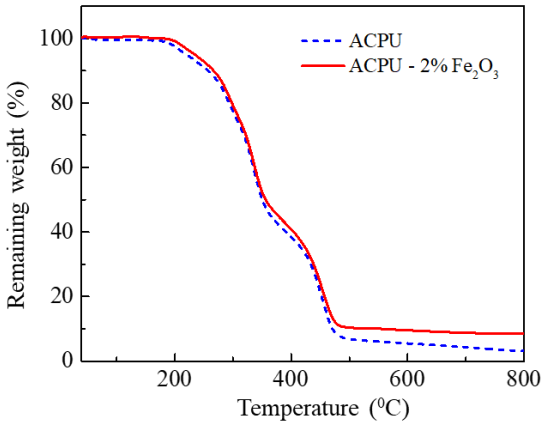

Figure 6. TGA curves of ACPU and ACPU-2 % Fe_2O_3 coating.

Table 3. TGA parameters of ACPU and ACPU-2 % Fe_2O_3 coatings.

Sample	**$T_{5\%}$ (^oC) (5 % loss in mass)**	**$T_{50\%}$ (^oC) (50 % loss in mass)**	**$T_{75\%}$ (^oC) (75 % loss in mass)**
ACPU	219.38	350.64	444.67
ACPU-2 %Fe_2O_3	234.47	356.77	448.13

As can be seen from Table 3, T_5 of ACPU-2 % Fe_2O_3 was 15 ^oC higher than that of ACPU. In other words, the degradation onset temperature of the ACPU-2 % Fe_2O_3 was higher than that of ACPU. It means that the thermal stability of ACPU-2 % Fe_2O_3 was higher than its counterpart. It was explained that Fe_2O_3 NPs, with small size, could fill the defects of the acrylic polyol coating, making the structure of ACPU-2 % Fe_2O_3 more compact, which limited heat transfer and oxygen penetration. As a result, the coating filled with Fe_2O_3 NPs had better thermal stability compared to the coating without NPs. These results are similar to other NPs such as rutile TiO_2 [19], SiO_2 [7], etc.

4. CONCLUSIONS

The effect of Fe_2O_3 NPs on the curing process and properties of acrylic polyol coatings was studied. The obtained results indicated that Fe_2O_3 NPs had an insignificant impact on the relative hardness and adhesion of acrylic polyol-based coatings but increased the abrasion resistance and impact resistance of the coatings at low contents (≤ 2 wt.%). However, the mechanical properties of the coatings decreased with increasing Fe_2O_3 content from 2 wt.% to 4 wt.%. The FE-SEM images confirmed that Fe_2O_3 NPs agglomerated in the polymer matrix of the coating loaded with 4 wt.% Fe_2O_3 NPs, while Fe_2O_3 NPs could be dispersed well in the polymer matrix of the coating filled with ≤2 wt.% Fe_2O_3 NPs. This may be the cause of reduced mechanical properties with increasing Fe_2O_3 NPs content from 2 wt.% to 4 wt.%. The effect of Fe_2O_3 NPs on the curing process and thermal stability of acrylic polyol-based coatings were also investigated. The hardening of the acrylic polyol-based coatings slowed down in the presence of 2 wt.% Fe_2O_3 NPs. However, Fe_2O_3 NPs improved the thermal stability of the acrylic polyol-based coatings. 2

wt.% Fe_2O_3 NPs increased the degradation onset temperature of the acrylic polyol-based coatings by 15 ^oC.

Acknowledgement. This research is funded by the Vietnam Academy of Science and Technology under grant number TDVLTT.03/21-23.

CRediT authorship contribution statement: **Do Truc Vy:** Investigation, Visualization**; Dao Phi Hung:** Methodology; **Nguyen Tuan Anh**: Writing-original draft; Data Curation; **Tran Dai Lam**: Writing - Review & Editing; **Nguyen Thien Vuong**: Conceptualization, Funding acquisition, Validation, Writing - Review & Editing.

Declaration of competing interest. The authors declare no competing interests.

REFERENCES

1. Nguyen-Tri P., Nguyen T. V. - Radically curable nanobased coatings (chapter 10), In: Nguyen -Tri P., Rtimi S. and Ouellet C.-Plamondon (Eds), Nanomaterials Based Coatings, Elsevier, 2019, pp. 1-35; DOI: 10.1016/B978-0-12-815884-5.00010-7.
2. Nguyen T. V., Nguyen T. P., Nguyen T. D., El Aidani R., Trinh V. T., Decker C. - Accelerated degradation of water borne acrylic nanocomposites used outdoor protective coatings, Polym. Degrad. Stab. **128** (2016) 65-76.
3. Nguyen T. V., Nguyen T. A., Nguyen T. H. - The Synergistic Effects of SiO_2 Nanoparticles and Organic Photostabilizers for Enhanced Weathering Resistance of Acrylic Polyurethane Coating. J. Compos. Sci. **4** (2020) 23. https://doi.org/10.3390/jcs4010023.
4. Nguyen T. V. - The role of rutile TiO_2 nanoparticles on weathering resistance of photocurable acrylate urethane coating, Vietnam J. Chem. **58** (2020) 314-320. https://doi.org/10.1002/vjch.2019000129
5. Nguyen T. M., Bui T. M. A., Nguyen T. V. - Acid and alkali resistance of Acrylic polyurethane/R-SiO_2, Vietnam J. Chem. **58** (1) (2020) 67-73. https://doi.org/10.1002/vjch.2019000124.
6. Hoang T. H. T., Hoang T. H., Nguyen T. V., Nguyen T. A. - The Alkaline Resistance of Waterborne Acrylic Polymer/SiO_2 Nanocomposite Coatings, J. Anal. Methods. Chem. (2022). https://doi.org/10.1155/2022/8266576.
7. Nguyen N. L., Dang T. M. L., Nguyen T. A., Ha H. T., Nguyen T. V. - Study on Microstructure and Properties of the UV Curing Acrylic Epoxy/SiO_2 Nanocomposite Coating, J. Nanomater. (2021). https://doi.org/10.1155/2021/8493201.
8. Do T. V., Ha M. N., Nguyen T. A., Ha H. T., Nguyen T. V. - Crosslinking, Mechanical Properties, and Antimicrobial Activity of Photocurable Diacrylate Urethane/ZnO-Ag Nanocomposite Coating, Adsorpt. Sci. Technol. (2021). https://doi.org/10.1155/2021/7387160
9. Nguyen T. V., Do T. V., Ngo T. D., Nguyen T. A., Le T. L., Vu Q. T., Pham T. L. and Tran D. L., Photocurable acrylate epoxy/ZnO–Ag nanocomposite coating: fabrication, mechanical and antibacterial properties, RSC Advances **12** (36) (2022) 23346-23355. doi:10.1039/D2RA03546D)
10. Nguyen T. V., Tran D. L., Nguyen T. A., Nguyen T. T. H., Dao P. H., Mac V. P., Do M. T., Nguyen T. M., and Dang T. M. L. - Ce-loaded silica nanoparticles in the epoxy

nanocomposite coating for anticorrosion protection of carbon steel, Anti-Corros. Method. Mater. **69** (2022) 514-523. https://doi.org/10.1108/ACMM-03-2022-2629

11. Nguyen T. V., Dao P. H., Nguyen T. A., Dang V. H., Ha M. N., Nguyen T. T. T., Vu Q. T., Nguyen N. L., Dang T. C., Nguyen P. T., Tran D. L., Lu L.T. - Photocatalytic degradation and heat reflectance recovery of water-borne acrylic polymer/ZnO nanocomposite coating, J. Appl. Polym. Sci. **137** (37) (2020) 49116. https://doi.org/10.1002/app.49116
12. Dao P. H., Nguyen T. V., Nguyen T. A., Doan T. Y. O., Hoang T. H., Le T. T., Nguyen P. T. - Acrylic Polymer/TiO_2 Nanocomposite Coatings: Mechanism for photo-degradation and Solar Heat Reflective Recovery, Mater. Chem. Phys. **272** (2021) 124984. https://doi.org/10.1016/j.matchemphys.2021.124984
13. Jin T., Kong F., Bai R., and Zhang R. - Anti-corrosion mechanism of epoxy-resin and different content Fe_2O_3 coatings on magnesium alloy, Front. Mater. Sci. **10** (4) (2016) 367-374. doi:10.1007/s11706-016-0357-5.
14. Chen Y., Wen S., Wang J., Wang G., Wang C., Wang Y., Li S., Zhang J. - Preparation of α-Fe_2O_3@TA@GO composite material and its anticorrosion performance in epoxy modified acrylic resin coatings, Prog. Org. Coat. **154** (2021) 105987. doi:10.1016/j.porgcoat.2020.105987.
15. Liu T., Liu Y., Ye Y., Li J., Yang F., Zhao H., and Wang L. - Corrosion protective properties of epoxy coating containing tetraaniline modified nano-α-Fe_2O_3, Prog. Org. Coat. **132** (2019) 455-467. doi:10.1016/j.porgcoat.2019.04.010.
16. Li J., Meng F., Liu L., Cui Y., Liu R., Zheng H., Wang F. - Effect of nano-Fe_2O_3/graphene oxide hybrids on the corrosion resistance of epoxy coating under alternating hydrostatic pressure, Corros. Commun. **5** (2022) 62-72. https://doi.org/10.1016/j.corcom.2022.03.003
17. Sultan S., Kareem K., and He L. - Synthesis, characterization and resistant performance of α-Fe_2O_3@SiO_2 composite as pigment protective coatings, Surface and Coatings Technology **300** (2016) 42-49. doi:10.1016/j.surfcoat.2016.05.010.
18. Nguyen T. V., Le X. H., Dao P. H., Decker C., and Nguyen T. P. - Stability of acrylic polyurethane coatings under accelerated aging tests and natural outdoor exposure: The critical role of the used photo-stabilizers, Progress in Organic Coatings **124** (2018) 137-146. https://doi.org/10.1016/j.porgcoat.2018.08.013
19. Nguyen T. V., Nguyen T. A., Dao P. H., Mac V. P., Nguyen A. H., Do M. T., and Nguyen T. H. - Effect of rutile titania dioxide nanoparticles on the mechanical property, thermal stability, weathering resistance and antibacterial property of styrene acrylic polyurethane coating, Advances in Natural Sciences: Nanoscience and Nanotechnology **7** (4) (2016) 045015. doi:10.1088/2043-6262/7/4/045015.